Supplementary Material: Synchronization of Degrade-and-Fire Oscillators via a Common Activator

William Mather,[1,2] Jeff Hasty,[3,4,5] and Lev S. Tsimring[5]

[1]*Department of Physics, Virginia Tech, 850 West Campus Dr., Blacksburg, VA 24061-0435*
[2]*Department of Biological Sciences, Virginia Tech, 1405 Perry St., Blacksburg, VA 24061-0406*
[3]*Department of Bioengineering, UCSD, 9500 Gilman Dr., La Jolla, CA 92093-0412*
[4]*Molecular Biology Section, Division of Biology, UCSD, 9500 Gilman Dr., La Jolla, CA 92093-0368*
[5]*BioCircuits Institute, UCSD, 9500 Gilman Dr., La Jolla, CA 92093-0328*

Contents

I. MODEL MOTIVATION AND APPROXIMATIONS

The motivation for the model used in the main text stems from a model studied in Ref. [1] which in turn was introduced to elucidate the mechanism of oscillations in synthetic gene circuits based on delayed self-repression [2]. In Ref. [1], we demonstrated (in both deterministic and stochastic contexts) how a short delay in transcriptional negative feedback can lead to long oscillatory periods. The deterministic model for the oscillator is written as a delay-differential equation (DDE) for a repressor concentration x

$$\frac{dx}{dt} = F(x_{\tau_1}) - \frac{\gamma x}{K + x}, \tag{S1}$$

where the synthesis rate of the repressor protein x at time t is characterized by the function $F(\cdot)$ that depends on the delayed value of the repressor concentration $x(t-\tau_1)$. The repressor degradation is assumed enzymatic and described by the usual Michaelis-Menten kinetics. Function $F(x)$ is assumed to be monotonically decreasing with its argument. For definiteness, we can consider the model

$$\frac{dx}{dt} = \frac{\alpha}{(1 + \frac{x_{\tau_1}}{C_1})^2} - \frac{\gamma x}{K + x}, \tag{S2}$$

which was studied in Ref. [1].

Several approximations were made to the oscillator model in Eq. S2 to arrive at the final model in the main text of this Letter. We determined in Ref. [1] that in the limit $K \to 0$, i.e. the zeroth-order degradation limit, followed by the limit where C_1 is sufficiently small but nonzero, i.e. the tight repression limit, the model in Eq. S2 exhibited sawtooth "degrade-and-fire" (DF) oscillations. These oscillations are characterized by short bursts of repressor production (the "fire" phase) of duration approximately $2\tau_1$, followed by subsequent degradation of accumulated repressor. We observed that the duration of the degradation phase can be much longer than the duration of the firing phase. These results were not strictly dependent on the limit $K \to 0$, though care must be taken to keep K sufficiently small to ensure robust oscillations.

In Ref. [1], we also considered the effect of an activator (a positive regulator) A on the dynamics of the oscillator. The corresponding model can be written as

$$\frac{dx}{dt} = \frac{\alpha}{(1+\frac{x_{\tau_1}}{C_1})^2}\frac{f^{-1}+\frac{A}{C_2}}{1+\frac{A}{C_2}} - \frac{\gamma x}{K+x} \tag{S3}$$

with $f > 1$ determining the positive feedback strength. In the main text of the present Letter, we effectively assume that A is much smaller than C_2, such that A influences dx/dt linearly

$$\frac{dx}{dt} \approx \frac{\alpha}{(1+\frac{x_{\tau_1}}{C_1})^2}\left(f^{-1}+(1-f^{-1})\frac{A}{C_2}\right) - \frac{\gamma x}{K+x} \tag{S4}$$

The activator A only influences the DDE in Eq. S4 during a firing event, i.e. when x_{τ_1} is small. In the limit of $K \to 0$ and $C_1 \to 0$, followed by the limit of $\tau_1 \to 0$ while $\alpha\tau_1$ remains fixed, a derivation similar to that in Ref. [1] then leads to a firing amplitude for the oscillator

$$P = \alpha\tau_1\left(f^{-1}+(1-f^{-1})\frac{A(0)}{C_2}\right) \tag{S5}$$

where A is evaluated at a firing event arbitrarily set to occur at time $t = 0$. It is trivial to rewrite Eq. S5 in the form

$$P = X_0 + \nu A(0) \tag{S6}$$

as in Eq. 3 of the main text.

Ref. [1] additionally investigated the influence of stochastic noise on DF oscillations, with the finding that the firing phase tended to generate most of the variability in amplitude and period of the oscillations. This was due to the amplitude of the firing phase being determined when repressor count is small (x is small) and thus noisy. Correspondingly, the model in the main text of this Letter only accounts for noise that occurs during firing rather than degradation. This firing noise was furthermore assumed to be white (uncorrelated between firing events), since the time between firing events can be long, i.e. comparable to or longer than a cell division period.

The magnitude and the distribution of fluctuations of firing amplitudes sensitively depend on the biochemical details of protein synthesis. For example, in Ref. [1], we were able to determine approximate relationships between firing variability ("noise strength") and other parameters of the system, e.g. mean firing amplitude, and to find its distribution (Poisson) for a particular stochastic model of firing kinetics. However, in the main text we make a simplifying assumption of the uniform distribution of firing amplitudes $[X_0 - \eta/2, X_0 + \eta/2]$ with magnitude η that is treated as an independent parameter. In the Main text we keep the mean firing amplitude X_0 fixed and vary η in the bifurcation analysis. In Section VI below we also consider the example of the multiplicative noise when η linearly depends on X_0.

II. SIMULATION DETAILS

Simulation of the coupled oscillator system was done as follows. A time step $dt = 0.01$ was chosen for the simulation, which is roughly 1/100 the magnitude of most rates. The oscillator with index n at simulation step m is represented by a variable $x_n(m)$, while the mean field coupling variable at simulation step m is represented by $A(m)$.

The update operation $A(m) \to A(m+1)$ uses the exact solution to the formula

$$\frac{dA}{dt} \;=\; \frac{1}{N}\sum_n x_n - \beta A \tag{S7}$$

assuming an integration time of dt, the initial condition $A(m)$, and the approximation that oscillator obeys the simple dynamics $dx_n/dt = -\gamma$. Thus, we do not assume that the oscillators "fire" when computing the update for $A(m)$. With each of these update steps, the value of $A(m)$ is stored in a queue data structure of sufficient length, since previous values of A will be needed to compute the delayed interaction.

The update for the oscillators initially computes the intermediate value $x_n(m) - \gamma\, dt$. If $x_n(m) - \gamma\, dt < 0$, this indicates a "firing" event, where an impulse is added to give $x_n(m) = x_n(m-1) - \gamma dt + X_0 + \nu A(m - m_\tau) + \tilde{\xi}$, where m_τ is the appropriate number of simulation steps such that $\tau = m_\tau\, dt$, and where $\tilde{\xi}$ is an independent (for each firing) uniform random variable distributed in $[-\eta/2, \eta/2]$.

Unless otherwise mentioned, a transient time of 1 000 000 steps are always performed before measuring system behavior. Statistics for trajectories over 20 000 subsequent iterations then are used to form the results in the main text.

III. STRONGLY SYNCHRONIZED SINGLE CLUSTER

A. Mean Field Solution

For the very low noise case $\eta \approx 0$, we consider the periodic solution of Eqs (3),(4) of the main text corresponding to a highly synchronized single cluster of Degrade-and-Fire (DF) oscillators. We will make the assumption that the period T satisfies $\tau < T$, which will considerably simplify the analysis. The case where $\tau > T$ can also be considered by iteration of the technique presented here.

The periodic solution can be found as follows. Write the periodic solution for the mean field of the oscillators as $x_s(t)$, and write the periodic solution for the coupling signal as $A_s(t)$. Suppose that a "firing" event occurs at $t = 0$, such that $x_s(-\epsilon) \approx 0$ and $x_s(\epsilon) = P_s$, for infinitesimal ϵ, and with $P_s \equiv X_0 + \nu A_s(-\tau)$. The solution for x_s in the vicinity of $t = 0$ is

$$x_s(t) \;=\; -\gamma t\ , \quad -T < t < 0 \tag{S8}$$

$$x_s(t) \;=\; P_s - \gamma t\ , \quad 0 < t < T \tag{S9}$$

Thus, $T = P_s/\gamma$. The dynamical equation for $A_s(t)$ is as before

$$\frac{dA}{dt} \;=\; x_s(t) - \beta A \tag{S10}$$

and can be solved for $t \in [-T, T]$ by knowledge of $x_s(t)$. In particular it can be shown

$$A_s(-\tau) \;=\; \frac{\gamma\,\tau}{\beta} + \frac{\gamma}{\beta^2} + \mathrm{e}^{\beta\,\tau}\left(A_s(0) - \frac{\gamma}{\beta^2}\right) \tag{S11}$$

$$A_s(T) \;=\; \frac{\gamma}{\beta^2} + \mathrm{e}^{-P_s\,\beta/\gamma}\left(A_s(0) - \frac{P_s}{\beta} - \frac{\gamma}{\beta^2}\right) \tag{S12}$$

Equation S11 can be used to determine an expression for $P_s \equiv X_0 + \nu A_s(-\tau)$, which in turn can be substituted into Eq. S12 as a consistency condition for the unknown $A_s(0) = A_s(T)$, which provides the periodic solution. A general analytic solution for $A_s(0)$ is not known to us, but the solution for $\nu = 0$ is simple, and it was be used as a starting point for numerical continuation schemes.

B. Linear Stability

Here we consider the dynamics of a single DF oscillator driven by a periodic mean field solution $A_s(t)$ with period T. Label the firing times for the driven oscillator as t_n for integer n. These times then obey the dynamics

$$t_{n+1} = t_n + \frac{X_0 + \nu A_s(t_n - \tau) + \tilde{\xi}_n}{\gamma} \tag{S13}$$

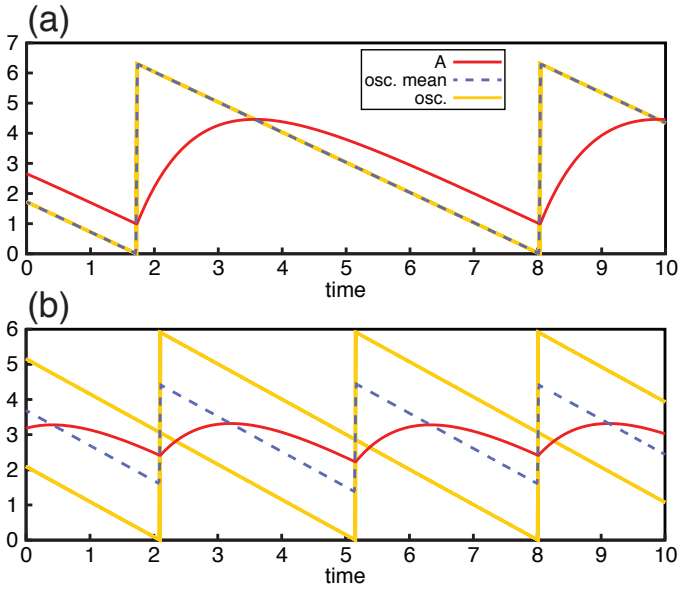

FIG. S1: Illustration of metastability, with plotted quantities similar to those in Fig. 1 of the main text, where "osc. mean" refers to the mean value $\langle x \rangle$, and "osc." refers to a randomly chosen set of 30 oscillators from the whole. A set of 1000 oscillators were started in a near perfect single cluster state, uniformly distributed in $[9.95, 10.05]$. Parameters were chosen to be $\gamma = 1$, $\beta = 1$, $X_0 = 5$, $\tau = 4$, $\nu = 0.3$, and $\eta = 0.01$. (If $\eta = 0$ instead, it can be shown that the single cluster state is stable with these parameters.) (a) After simulation for 10 000 time units, the system remains in the single cluster state. (b) After simulation for 500 000 time units, the system was found in the two cluster state, more consistent with the results in Fig. 2c,d of the main text.

where each $\tilde{\xi}_n$ is an independent uniform random variable distributed in $[-\eta/2, \eta/2]$, and η is assumed in this case to be small. If the entrained oscillator has the same parameters as the mean field ensemble in the previous subsection, then if we assume each firing time t_n is near the n^{th} firing time, nT, of the ensemble, we can define the deviation $\delta t_n = t_n - nT$. Then conditional on known t_n, the entrained oscillator obeys to lowest order

$$\begin{aligned}
\delta t_{n+1} - \delta t_n &= t_{n+1} - t_n - T && \text{(S14)}\\
&= \frac{X_0 + \nu A_s(t_n - \tau) + \tilde{\xi}_n}{\gamma} - T && \text{(S15)}\\
&= \frac{X_0 + \nu A_s(nT + \delta t_n - \tau)}{\gamma} - T + \frac{\tilde{\xi}_n}{\gamma} && \text{(S16)}\\
&\approx \frac{\nu}{\gamma}\frac{\partial A_s}{\partial t}(nT - \tau)\,\delta t_n + \frac{\tilde{\xi}_n}{\gamma} && \text{(S17)}
\end{aligned}$$

By periodicity of $A_s(t)$

$$\delta t_{n+1} \approx \left(1 + \frac{\nu}{\gamma}\frac{\partial A_s}{\partial t}(-\tau)\right)\delta t_n + \frac{\tilde{\xi}_n}{\gamma} \qquad \text{(S18)}$$

Neglecting fluctuations, δt is stable towards zero if

$$\left|1 + \frac{\nu}{\gamma}\frac{\partial A_s}{\partial t}(-\tau)\right| < 1\ , \quad \text{(stability, no fluctuations)} \qquad \text{(S19)}$$

Since A_s tends to be decaying near the time before the next firing, we expect $\frac{\partial A_s}{\partial t}(-\tau) < 0$ for τ not too large, and so we expect the single cluster solution to be stable for a range of parameters.

The condition Eq. S19 can be used to demonstrate stability of a single cluster for regions of parameter space not typically displaying single cluster oscillators. For instance, consider Fig. 2c,d of the main text. These panels use the parameters $\gamma = 1$, $X_0 = 5$, $\beta = 1$, $\tau = 4.0$, with ν and η variable. Numerical investigation of the stability for the

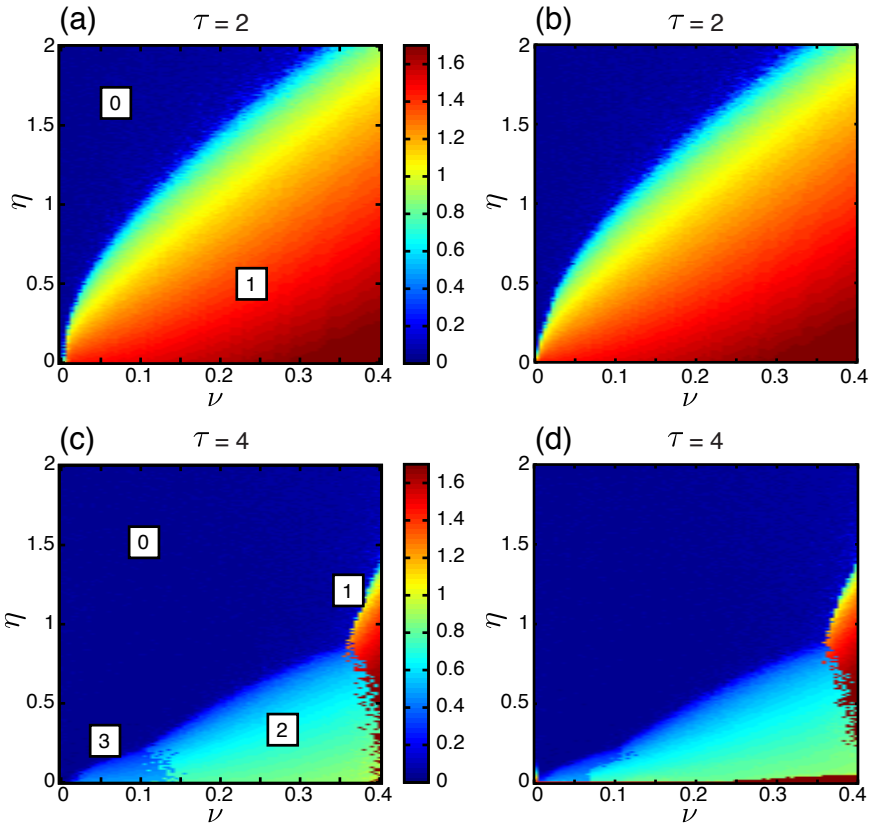

FIG. S2: Illustration of low sensitivity to initial conditions for Fig. 2a,c of the main text. Panels (a) and (c) are identical to panels (a) and (c) in Fig. 2 of the main text (see main text Fig. 2 caption for details). Panel (b) is an identical scan of simulations as in panel (a), but with all oscillators initialized at the same value, $x_n = 10$. Negligible differences are noticed between these panels. Similarly, panel (d) is panel (c) with the initial condition $x_n = 10$. In this case, a band of single cluster oscillations for small η but large ν are observed in (d) but not in (c). We believe these are mostly metastable states. Also, some distortion of the boundary between the two cluster and three cluster regions can be noticed.

single cluster solution when $\eta = 0$ suggests $\nu > 0.1882197809$ is stable for the range of ν considered in the plot. This range is beyond where single clusters are observed in Fig. 2c of the main text. Simulation of this solution for finite η may explain why; these solutions may tend to be metastable. Fig. S1 illustrates this point.

Despite the potential complexity associated with exploring a system with multiple metastable states, we do not find that our results are very sensitive to the initial condition used. Figure S2 compares the results from the main text, which used an initial condition reminiscent of the asynchronous state, to an initial condition where all oscillators are identical. Only subtle differences are observed, including a new narrow band of single cluster oscillations for η small and ν large. These oscillations are the metastable oscillations discussed in the previous paragraph.

IV. STEADY STATE SOLUTION AND LINEAR STABILITY ANALYSIS IN THE CONTINUUM LIMIT: GENERAL TREATMENT

A. Steady State

The equations governing dynamics in the continuum limit are

$$\partial_t f(x,t) = \gamma \partial_x f(x,t) + \gamma g(x, A_\tau) f(0,t) \tag{S20}$$

$$\frac{dA}{dt} = \int_0^\infty x\, f(x,t)\, dx - \beta A \tag{S21}$$

where $A_\tau = A(t-\tau)$ is a delayed variable. The steady state is defined by the solution to the coupled equations (subscript "0" indicates steady state in this context)

$$0 = \partial_x f_0(x) + g(x, A_0) f_0(0) \tag{S22}$$

$$0 = \int_0^\infty x\, f_0(x)\, dx - \beta A_0 \tag{S23}$$

Equation S22 can be solved conditional on the steady state value A_0

$$f_0(x) = f_0(0) \left(1 - \int_0^x g(x, A_0)\, dx\right) \tag{S24}$$

which ensures that $f_0 \to 0$ as $x \to \infty$ if $\int_0^\infty g(x,A)dx = 1$. The value of $f_0(0)$ can be fixed by the condition $\int_0^\infty f_0(x)dx = 1$. We must then solve the consistency condition for A_0, from Eq. S23

$$f_0(0) \int_0^\infty x' \left(1 - \int_0^{x'} g(x, A_0)\, dx\right) dx' = \beta A_0 \tag{S25}$$

which can be analytically computed given particular choices for $g(x, A)$.

B. Linear Stability

Linear stability from this zeroth order solution can be done via a perturbation expansion. To lowest order

$$f(x,t) = f_0(x) + f_1(x) e^{\lambda t} \tag{S26}$$

$$A = A_0 + A_1 e^{\lambda t} \tag{S27}$$

where f_1 and A_1 are small. Substituting this into Eqs. S20–S21 and expanding to linear order provides

$$\partial_x f_1(x) = \left(\frac{\lambda}{\gamma}\right) f_1(x) - g(x, A_0)\, f_1(0) - \frac{\partial g}{\partial A}(x, A_0)\, f_0(0)\, A_1 e^{-\lambda\tau} \tag{S28}$$

$$(\lambda + \beta)\, A_1 = \int_0^\infty x f_1(x)\, dx \tag{S29}$$

where we must satisfy the condition $f_1(\infty) = 0$.

V. STEADY STATE SOLUTION AND LINEAR STABILITY ANALYSIS IN THE CONTINUUM LIMIT: UNIFORM RANDOM NOISE

A. Steady State

A particular choice for $g(x, A)$ can greatly simplify the analysis for synchronized DF oscillators. One of the simplest such choices is a uniform noise distribution within a range $(-\eta/2, \eta/2)$ which corresponds to

$$g(x, A) = \frac{\Theta(X_0 + \nu A - \eta/2) - \Theta(X_0 + \nu A + \eta/2)}{\eta} \tag{S30}$$

where $\Theta(\cdot)$ is the Heaviside function. Define $x_1 \equiv P - \eta/2$ and $x_2 \equiv P + \eta/2$, where $P \equiv X_0 + \nu A_0$ is the zeroth order firing amplitude. To simplify the resulting expressions in this section, we rescale time to set $\gamma = 1$. Recovering expressions for $\gamma \neq 1$ is straightforward.

The zeroth order solution to this particular problem can be derived from application of Eqs. S24–S25. Equation S24 has the piecewise linear solution

$$f_0(x) = \frac{2}{x_2 + x_1} = \frac{1}{P} \quad , \; x \leq x_1 \tag{S31}$$

$$f_0(x) = \frac{2(x_2 - x)}{(x_2 + x_1)(x_2 - x_1)} = \frac{P + (\eta/2) - x}{P\,\eta} \quad , \; x_1 \leq x < x_2 \tag{S32}$$

$$f_0(x) = 0 \quad , \; x \geq x_2 \tag{S33}$$

Using this solution, the mean value of x is calculated to be

$$\int_0^\infty x\, f_0(x,t)\, dx = \frac{P}{2} + \frac{\eta^2}{24\, P} \tag{S34}$$

Consistency of the steady state condition (Eq. S25) then can be expressed as

$$\beta A_0 = \frac{P}{2} + \frac{\eta^2}{24\, P} \tag{S35}$$

or using the definition $P = X_0 + \nu A_0$

$$\left(\frac{\beta}{\nu}\right)(P - X_0) = \frac{P}{2} + \frac{\eta^2}{24\, P} \tag{S36}$$

which is a quadratic equation for P with a single physical solution

$$P = \frac{\beta\, X_0}{2\,\beta - \nu} + \frac{1}{6}\, \frac{\sqrt{36\,\beta^2 {X_0}^2 + 6\,\eta^2\nu\,\beta - 3\,\eta^2\nu^2}}{2\,\beta - \nu} \tag{S37}$$

This solution is divergent at $\nu = 2\beta$ and unphysical for $\nu \geq 2\beta$, which is a result of the simplistic functional form $X_0 + \nu A$ for the firing amplitude. A more realistic firing amplitude function would include saturation, e.g. being $(X_0 + \nu A)/(1 + \kappa A)$ for some $\kappa > 0$, which would prevent this divergent behavior.

B. Linear Stability

The linear stability analysis follows from Eqs. S28–S29. Firstly, notice that

$$\frac{\partial g}{\partial A}(x, A_0) = -\frac{\nu}{\eta}\left(\delta(x - x_1) - \delta(x - x_2)\right) \tag{S38}$$

where $\delta(x)$ is the Dirac delta function. This expression for $\partial g/\partial A$ substituted into Eq. S28 leads to the jump conditions

$$f_1(x_1 + \epsilon) - f_1(x_1 - \epsilon) \;=\; \left(\frac{f_0(0)}{\eta}\right)\nu A_1 e^{-\lambda\tau} = \left(\frac{1}{P\,\eta}\right)\nu A_1 e^{-\lambda\tau} \tag{S39}$$

$$f_1(x_2 + \epsilon) - f_1(x_2 - \epsilon) \;=\; -\left(\frac{f_0(0)}{\eta}\right)\nu A_1 e^{-\lambda\tau} = -\left(\frac{1}{P\,\eta}\right)\nu A_1 e^{-\lambda\tau} \tag{S40}$$

for infinitesimal positive ϵ. Away from these points, $g(x, A_0)$ is piecewise constant, and $\partial g/\partial A(x, A_0) = 0$, leading to

$$\frac{f_1(x)}{f_1(0)} \;=\; e^{\lambda x} \quad,\; x < x_1 \tag{S41}$$

$$\frac{f_1(x)}{f_1(0)} \;=\; \frac{1}{\lambda\eta} + \left(e^{\lambda x_1} + \left(\frac{1}{P\,\eta}\right)\nu\,\zeta\, e^{-\lambda\tau} - \frac{1}{\lambda\eta}\right) e^{\lambda(x - x_1)} \quad,\; x_1 < x < x_2 \tag{S42}$$

where $\zeta \equiv A_1/f_1(0)$. We then have to satisfy the consistency condition $f_1(x_2 + \epsilon) = 0$, which after minimal algebraic manipulation is

$$0 \;=\; e^{\lambda(P + \eta/2)} + \left(e^{\lambda\eta} - 1\right)\left(\frac{\nu\,\zeta\, e^{-\lambda\tau}}{P\,\eta} - \frac{1}{\lambda\eta}\right) \tag{S43}$$

Equations S41–S42 can also be used to compute piecewise the required integral $\int_0^\infty x\, f_1(x)\, dx$ in Eq. S29, which leads to another equation that must be solved for the linear stability problem. Finally, we have a pair of equations to be solved simultaneously for our eigenvalue problem

$$0 \;=\; e^{\lambda(P + \eta/2)} + \left(e^{\lambda\eta} - 1\right)\left(\frac{\nu\,\zeta\, e^{-\lambda\tau}}{P\,\eta} - \frac{1}{\lambda\eta}\right) \tag{S44}$$

$$0 \;=\; (\lambda + \beta)\,\zeta - \frac{\nu\,\zeta\, e^{-\lambda\tau} + P^2}{\lambda P} \tag{S45}$$

We will leave derivation of Eq. S45 to the reader.

A special case of Eqs. S44–S45 is in the case with no coupling, i.e. $\nu = 0$. Then we only need to solve

$$0 \;=\; \eta\, e^{\lambda(P+\eta/2)} - \frac{e^{\lambda\eta}-1}{\lambda} \tag{S46}$$

Equation S46 describes the spectrum for an ensemble of stochastic, uncoupled oscillators. We can expand Eq. S46 in η to find

$$0 = \left(\mathrm{e}^{\lambda P}-1\right)\eta + \frac{1}{2}\lambda\,\left(\mathrm{e}^{\lambda P}-1\right)\eta^2 + O\left(\eta^3\right) \tag{S47}$$

To lowest order, Eq. S47 implies

$$\lambda \approx \frac{2\pi i\, n}{P} \quad ,\ (\nu = 0,\ \eta \text{ small},\ \text{integer } n) \tag{S48}$$

From the eigenfunction expressions Eqs. S41–S42, we notice that each integer n in Eq. S48 corresponds (approximately) to a Fourier mode with n oscillations. Thus, the branch in the eigenvalue spectrum corresponding to integer n should be the branch corresponding to an n-cluster perturbation, where n clusters of oscillators break the asynchronous state. This is indeed what we find in our numerical simulations (see Fig. 2 in the main text).

In our computational investigations, we solve Eqs. S44–S45 by numerical continuation of known analytic solutions in the limit $\nu = 0$ and η small but finite (see Eq. S48). We then plot the contours when the real value of λ crosses zero. A variety of such bifurcation diagrams can be found in Supplementary Figs. S4–S5 (found at the end of this document). In particular, notice in Supplementary Figure S5 that a large region only containing the single cluster synchronous state often exists when η is sufficiently large.

VI. MULTIPLICATIVE NOISE MODELS

Most of the analysis in this Letter assumes that a single parameter η is sufficient to specify the firing noise strength for all oscillators in the system. However, we mentioned at the end of Section I that in real gene circuits, the noise is expected to be constrained in some way, in particular, the noise magnitude can be related to mean firing amplitude. In the main text, we kept X_0 fixed, and therefore changing η without changing X_0 can be thought of as changing the parameters of a specific functional relationship between X_0 and η (for example, the relative contributions of transcriptional and translational noise). However, one can also study the bifurcation diagram for a fixed function $\eta(X_0)$ by varying X_0. In this section, we present our calculations for a simple multiplicative noise model in which $\eta = \rho X_0$, with a new parameter, the *relative* noise strength ρ. In the corresponding simulations and the bifurcation analysis, we vary X_0 for several fixed ρ. However, to facilitate the comparison with the main text, we as before present them in the plane (ν, η).

Sample results for a model with given relative noise strength are presented in Fig. S3, which can be directly compared to Fig. 2 in the main text. Further exploration of the mode structure for these models appears in Fig. S6 at the end of this document. Based on these results, we can make a number of observations. Firstly and not surprisingly based on other results in this Letter, cluster dynamics in discrete simulations matches and therefore can be predicted by the mode stability analysis about the asynchronous state. Secondly, unlike the additive noise case, we find multiple bands of values for η where the first mode is unstable (and similarly for higher modes, results not shown). This is likely due to resonance effects: in the multiplicative noise case scanning η corresponds to scanning X_0 and with it changing the natural period of the underlying oscillators. This period may then resonate with the timescale τ for the global feedback delay. Finally, greater relative noise magnitude tends to decrease the complexity of the mode bifurcation diagram over a given a range of ν (Fig. S6).

A related but much less trivial modification of our model would be to suppose that the firing noise strength η depends *instantaneously* on the current mean firing amplitude $P = X_0 + \nu A$:

$$\eta = \rho P = \rho\,(X_0 + \nu A) \tag{S49}$$

(we as before assumed a linear dependence between η and P).

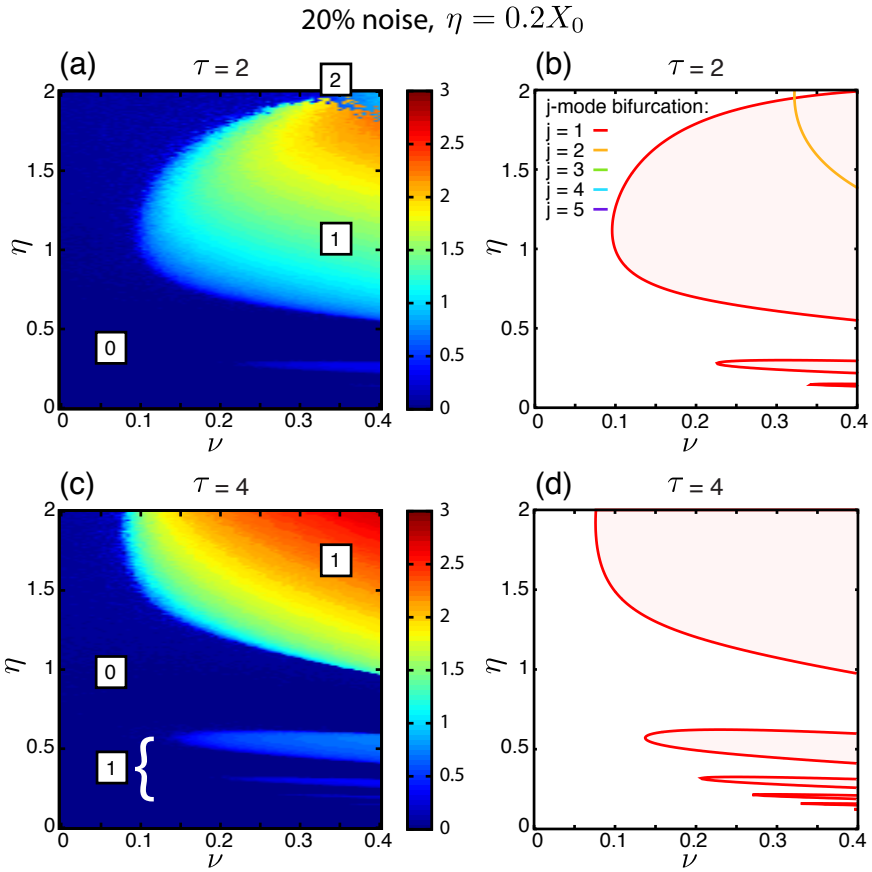

FIG. S3: Entirely analogous to Fig. 2 in the main text, but for the "multiplicative noise" case with $\eta = 0.2X_0$, i.e. 20% noise. (a) For $\tau = 2$, the standard deviation (over time) of the mean oscillator value $\langle x \rangle$ for 1000 oscillators. Boxed numerals indicate the number of clusters associated with the given region of parameter space. Other parameters are $\gamma = 1.0$ and $\beta = 1.0$. (b) Associated linear stability analysis of the continuum asynchronous state with respect to the mode j, calculated up through the fifth mode (note that we did not detect instability of modes $3 - 5$ in these particular plots). Regions *right* of the presented lines are unstable to growing oscillations of the density function. (c) and (d) are the same as (a) and (b), respectively, but for $\tau = 4$. The "speckling" between boundaries in part (a) is consistent with multistability, as suggested by coexistence of several unstable modes in part (b). Refer to Fig. S6 for a more complete exploration of mode structure.

Our preliminary results (not shown) suggest that for the values of parameters considered in our investigation, the qualitative dynamics of the model obeying Eq. S49 match the model where η is a constant across all cells. This might be expected for weak coupling, i.e. $\nu A \ll X_0$, since then $\eta \approx \rho X_0$, which is the example discussed above. We leave for future studies to explore the dynamics of the coupled DF oscillators with multiplicative noise more thoroughly.

[1] W. Mather, M. Bennett, J. Hasty, and L. Tsimring, Physical Review Letters **102**, 68105 (2009).
[2] J. Stricker, S. Cookson, M. R. Bennett, W. H. Mather, L. S. Tsimring, and J. Hasty, Nature **456**, 516 (2008).

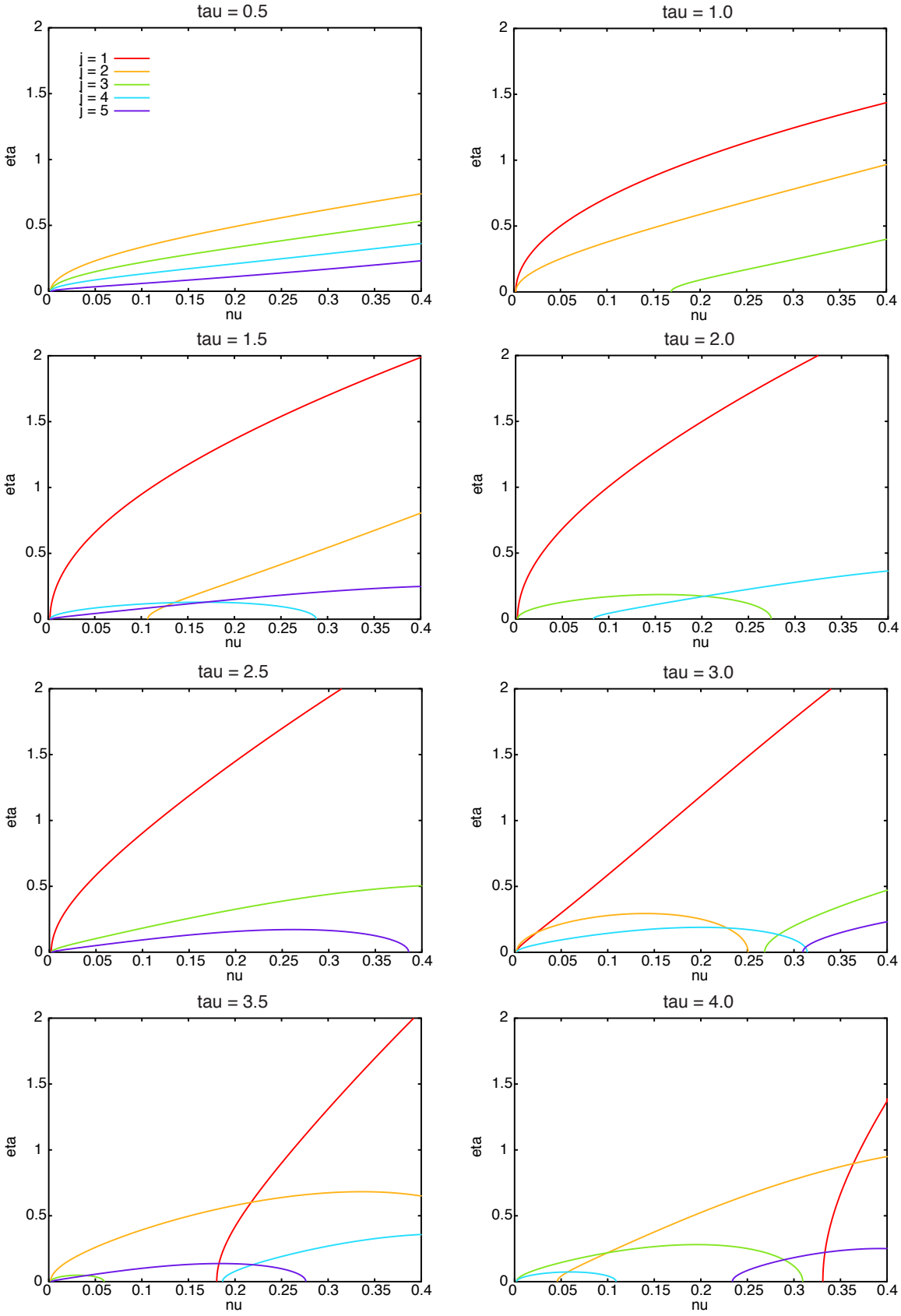

FIG. S4: A more complete linear stability analysis that augments Fig. 2b,d of the main text. Plotted is the stability of the j-cluster perturbation away from the homogenous state. Regions *below* the respective lines are unstable with respect to the mode perturbation.

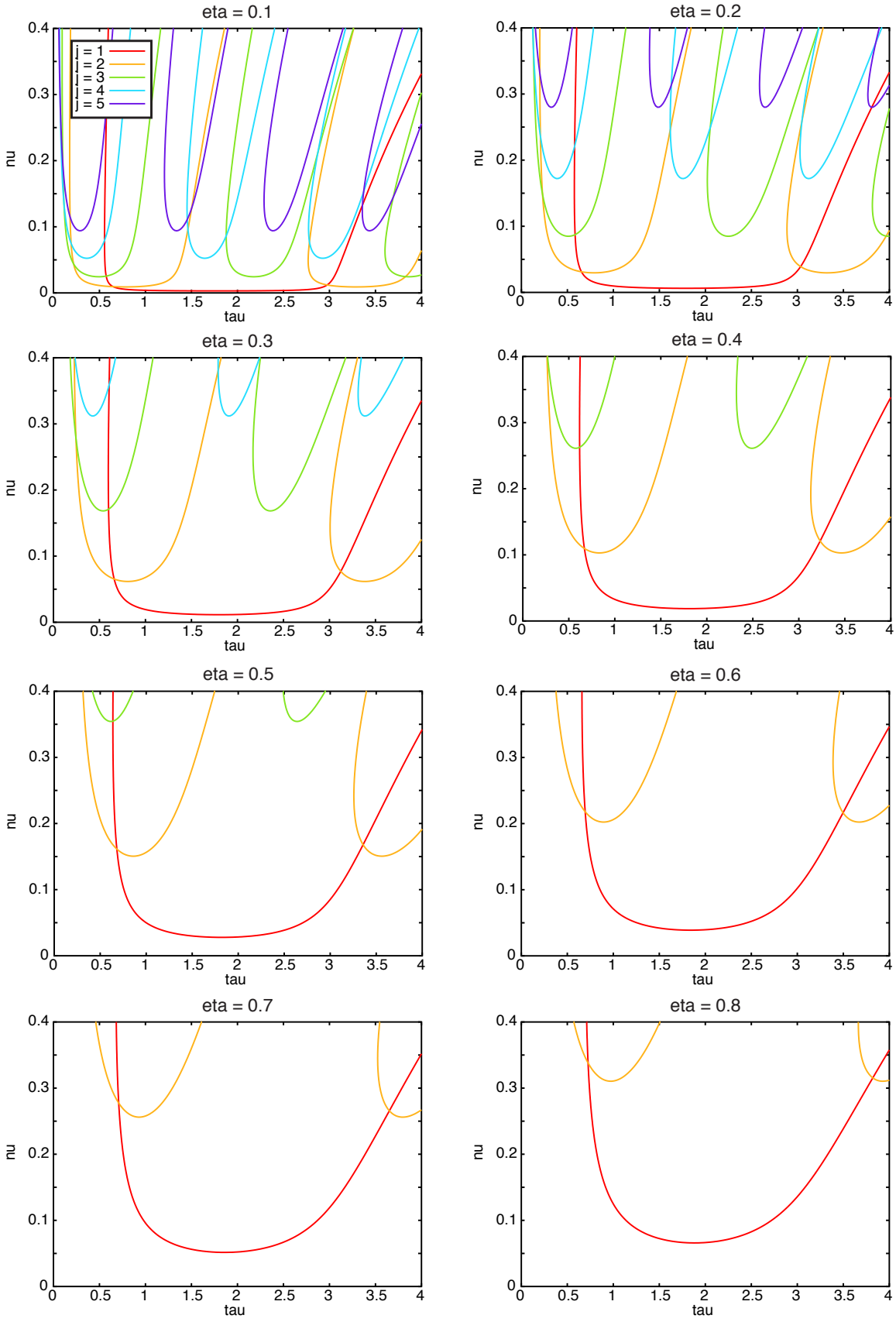

FIG. S5: A more complete linear stability analysis that augments Fig. 3 in the main text. Plotted is the stability of the j-cluster perturbation away from the homogenous state. Regions roughly *above* the respective curves are unstable with respect to the mode perturbation.

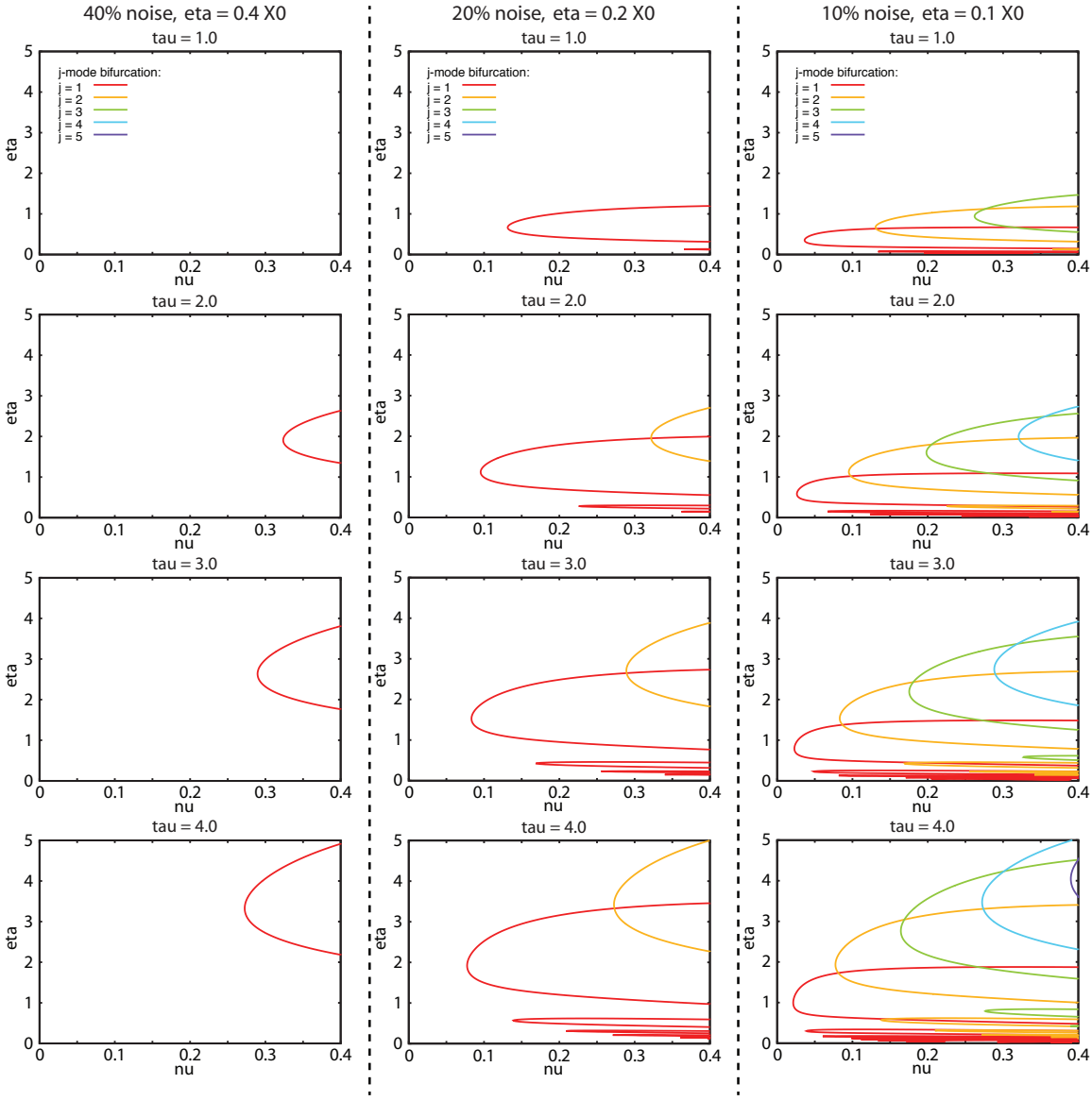

FIG. S6: Entirely analogous to Fig. S3b,d, but for a wider array of parameters. Presented is the associated linear stability analysis of the continuum asynchronous state with respect to the mode j, calculated through the fifth mode. Regions *right* of the presented lines are unstable to growing oscillations of the density function. Vertical columns share a common relative noise strength: (left) 40% noise ($\eta = 0.4X_0$), (middle) 20% noise ($\eta = 0.2X_0$), (right) 10% noise ($\eta = 0.1X_0$).